Themis: A Network Bandwidth-Aware Collective Scheduling Policy for Distributed Training of DL Models

Saeed Rashidi*, William Won*, Sudarshan Srinivasan[†], Srinivas Sridharan[‡], and Tushar Krishna*

*Georgia Institute of Technology, Atlanta, GA, USA

[†]Intel, Bangalore, India

[‡]Facebook, Menlo Park, USA

saeed.rashidi@gatech.edu, william.won@gatech.edu, sudarshan.srinivasan@intel.com, ssrinivas@fb.com, tushar@ece.gatech.edu

Abstract—The continuous growth in both size and training data for modern Deep Neural Networks (DNNs) models has led to training tasks taking days or even months. Distributed training is a solution to reduce training time by splitting the task across multiple NPUs (e.g., GPU/TPU). However, distributed training adds communication overhead between the NPUs in order to synchronize the gradients and/or activation, depending on the parallelization strategy. In today's datacenters, for training at scale, NPUs are connected through multi-dimensional interconnection links with different bandwidth and latency. Hence, keeping all network dimensions busy and maximizing the network BW is a challenging task in such a hybrid network environment, as this work identifies. We propose Themis, a novel collective scheduling scheme that dynamically schedules collectives (divided into chunks) to balance the communication loads across all dimensions, further improving the network BW utilization. Our results show that on average, Themis can improve the network BW utilization of single All-Reduce by $1.88 \times (2.92 \times \text{max})$, and improve the end-to-end training iteration performance of real workloads such as ResNet-50, GNMT, DLRM, and Transformer-1T by $1.49 \times (1.96 \times \text{max})$, $1.41 \times (1.81 \times \text{max})$, $1.42 \times (1.80 \times \text{max})$, and $1.35 \times (1.78 \times \text{max})$, respectively.

I. INTRODUCTION

Deep Neural Networks (DNNs) are constantly growing in demand due to their vast applicability in different areas such as computer vision [20], language modeling [39], recommendation systems [28], etc. In order to improve accuracy and enable emerging applications, the general trend has been towards an increase in both model size and the training dataset [14]. This makes the task of training these DNNs extremely challenging, requiring days or even months if run on a single accelerator [23], [38]. For e.g., in 2020, OpenAI set the record for training one of the largest NLP models ever, GPT-3, with 175B parameters. The training required 355 GPU years, or the equivalent of 1,000 GPUs working continuously for more than four months [3]. By 2021 we have already moved to training 1 Trillion parameter models as Google recently demonstrated [5].

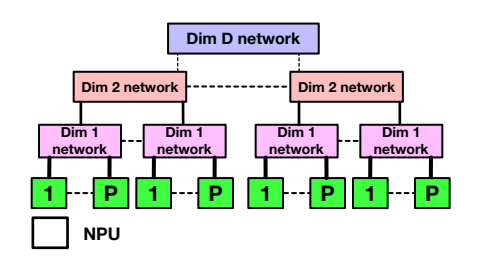
Distributed Training Platforms. The challenge of training AI models has opened up a sub-field of systems research specifically aimed at designing efficient *distributed* accelerator platforms. These platforms are built by first connecting tens of

high-performance accelerators (e.g., GPUs or TPUs, which we call Neural Processing Units (NPU) in this work for the sake of generality) with high-bandwidth proprietary interconnects (e.g., NVlink) and then scaling these clusters via datacenter networks (e.g., ethernet or InfiniBand). Examples of such platforms include Google's Cloud TPU [2], NVIDIA DGX [9], Intel Habana [7], and so on. Fig. 1(a) shows the abstraction of a such multi-dimensional network. Note that the NPU connectivity to each network dimension could be through dedicated links per each dimension (e.g., torus in Fig. 1.b or by interconnecting previous dimension switches (e.g., hierarchical switch in Fig. 1.c). In any case, these topologies form separate physical dimensions. To leverage the compute and networking capabilities of these platforms, the training workload (model + dataset) needs to be sharded across the accelerators via a parallelization strategy. The two popular parallelization strategies are: (i) data-parallel, where a mini-batch is split, and (ii) model parallel, where a model is divided across NPUs. Recent efforts have also looked into hybrid [28] and pipelined [21], [19] parallelization strategies.

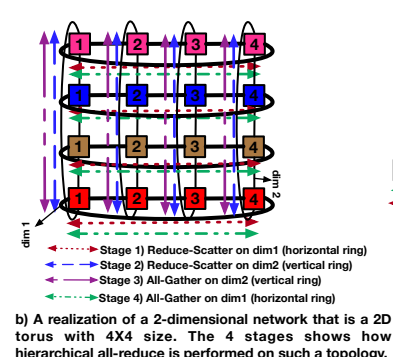
Communication. One of the biggest challenges with getting good performance out of these platforms is communication¹, as several previous studies have shown [24], [26], [36], [27], [35]. This is because, no matter what parallelization strategy is used, there is inevitable communication between the NPUs to exchange gradients and/or activations. Further, a high ratio of communication-to-computation in many DNN training workloads [26] makes them extremely difficult to scale, since communication becomes the bottleneck factor, diminishing the benefits of scaling. This problem in fact gets exacerbated as compute becomes more efficient [8], [34].

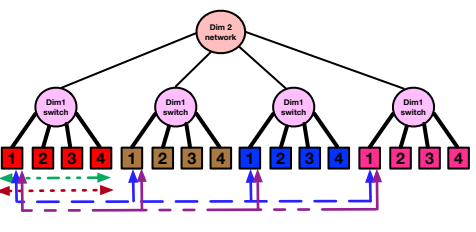
In this work, we identify a challenge with hierarchical training platforms, namely network bandwidth (BW) efficiency. Specifically, these hierarchical topologies are forced to use

¹There are two main methods to handle communication: (i) through a centralized parameter server, or (ii) using explicit NPU-to-NPU communication to exchange data by using collective communication patterns (e.g., All-Reduce. Discussed in detail in Sec. II) [34]. In this paper, we focus on the second approach, as it is more scalable and also has lower overhead [26].



a) A generic form of a multi-dimensional NPU network with D dimensions





c) A realization of a 2-dimensional network that is a hierarchical switch with AY4 size. The 4 stages shows how hierarchical allreduce is performed on such a topology. Note that here only communication pattern of the leftmost NPU is completely shown. The rest are not displayed for clarity reason

Fig. 1: An example of a distributed training platform with a multi-dimensional interconnection network in datacenters. As indicated by thicker lines in the figure, usually the lower dimensions have higher BW (There are some exceptions such as Intel Habana Gaudi [7], [4] platform, where multiple dimensions can be configured to have the same BWs).

interconnection links with different bandwidths and latencies in each dimension (constrained by technology), as shown in Fig. 1. For e.g., the aggregated bandwidth of NVlinks being used in lower dimensions is $6 \times$ higher than that of ethernet used at higher dimensions [30]. To account for this mismatch, state-of-the-art collective communication (e.g., All-Reduce) scheduling algorithms use hierarchical algorithms, breaking the collective into phases (e.g., All-Reduce broken into Reducescatter and All-gather) and chunks from various phases of the collective moving through the network dimensions in a pipelined manner. The goal of these algorithms is to reduce the volume of traffic as we go up dimensions, as Fig. 1(b) and (c) illustrate. Unfortunately, as we identify in this work, a mismatch between the chunk size and bandwidth per dimension can lead to unbalanced pipeline stages. This in turn means that the overall communication performance is dictated by the slowest stage, leading to network BW under-utilization in other dimensions of the topology.

Fig. 2 quantifies this effect. It shows the overall (normalized) training time reduction as the avg. network BW utilization increases for three different DNNs with high ratio of communication to compute (Sec. V discusses the experimental methodology and data in more detail). According to Fig. 2, the runtime curves are relatively similar across the three training workloads. This is because these workloads are communication bound, hence, their runtime is mainly dictated by the underlying network performance. Fig. 2 also shows baseline multi-rail collective-communication scheduling fails to utilize the available BW efficiently due to unbalanced stage latencies, reaching to the average BW utilization of 55.6%, when averaging across all the workloads and topologies. In particular, if the ideal utilization (100%) can be achieved, the training performance on average can be improved by $1.51\times$, $1.44\times$, and $1.37\times$ over the baseline for ResNet-50, GNMT and Transformer-1T, respectively.

In this paper, we propose Themis, a novel chunk scheduling scheme that dynamically gives different chunks distinct pipeline schedules to maximize the utilization of all network dimensions. We leverage the insight that algorithmically there is no strict ordering to perform Reduce-Scatter or All-Gather stages. In

other words, to perform Reduce-Scatter/All-Gather stages a chunk may start at any network dimension and traverse dimensions in any order. The only synchronization point is that the Reduce-Scatter stage must be completed before starting All-Gather. Themis uses this fact and schedules chunks differently to balance loads of all network dimensions.

In short, we make the following contributions:

- This is the first work, to the best of our knowledge, exploring the problem of multi-rail collective-communication scheduling at scale (1024 NPUs in this case) over hierarchical topologies.
- We identify the problem of unbalanced stage latencies in multi-rail collective scheduling algorithms which rely on fixed pipeline schedules for all chunks of data.
- We propose Themis, a novel chunk scheduling scheme for multi-dimensional networks that dynamically schedules the chunks to maximize utilization of each dimension.
- Our results (see Sec. V for methodology) show that, on average, Themis reduces All-Reduce time by 1.88× and achieves 94.61% BW utilization. This improves end-to-end training latency for ResNet-50, GNMT, DLRM, and Transformer-1T by 1.49× (1.96×max), 1.41× (1.81×max), 1.42× (1.80×max), and 1.35× (1.78×max), respectively.

II. BACKGROUND & RELATED WORKS

A. Collective Communication Patterns

Communication is the inevitable overhead to pay in distributed training workloads. The exact communication patterns each training workload requires depend on the parallelization strategy, and also the communication mechanism (i.e. parameter server vs. explicit NPU-to-NPU). When using the explicit NPU-to-NPU communication mechanism, All-Reduce is the most dominant pattern observed in distributed training [24]. For example, in the case of a data-parallel parallelization strategy, each NPU works on a subset of the global mini-batch in each iteration, thus, their calculated weight gradients must be globally reduced (i.e. All-Reduce) before updating the weights and starting the new training iteration.

All-Reduce can be broken into a Reduce-Scatter followed by an All-Gather communication patterns. Fig. 3.a shows the

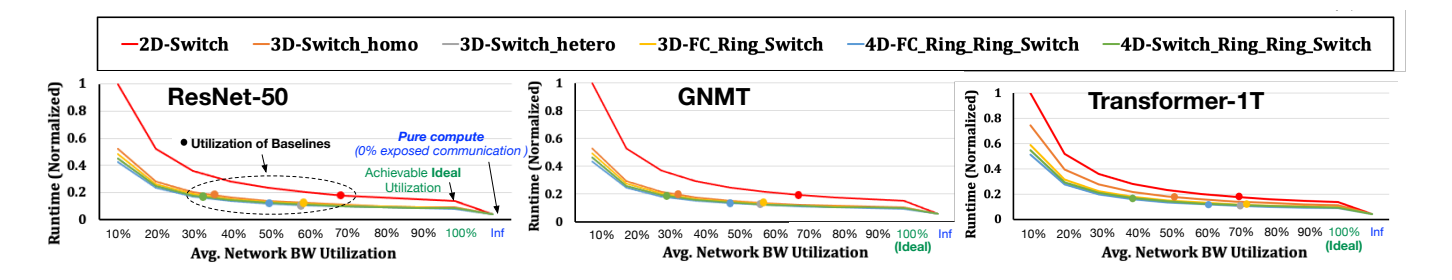


Fig. 2: Normalized runtime vs. average BW utilization for three different-sized DNN training workloads running on six different topologies (please see Sec. V for full description of workloads and topologies). The DNNs are: (i) ResNet-50, (ii) GNMT, and (iii) Transformer-1T (1 Trillion params). The BW utilization is obtained only during the time when there are communication operations issued by the workload (excluding the times when there is no pending communication operation). All runtimes are normalized to the slowest topology (i.e. 2D-Switch) runtime at 10% BW utilization. The bold dots show the baseline BW utilization. Inf (i.e., infinite) BW is when communication overhead is 0% and runtime stems from compute only. Ideal represents the achievable runtime if the network BW aross all dimensions is fully utilized.

mathematical implications of these patterns performed on four NPUs. Reduce-Scatter performs reduction operation among initial data such that at the end, each NPU holds a portion of the globally reduced data. All-Gather, on the other hand, broadcasts data residing on each NPU to all other NPUs. Therefore, it is clear that when performing Reduce-Scatter/All-Gather on P participating NPUs, the data size residing on each NPU shrinks/multiplies by $P\times$.

B. Basic Collective Communication Algorithms

Each of the collective communication patterns described in Sec. II-A can be performed through different collective communication algorithms. For example, tree-based [31], ring-based [16], and halving-doubling [18] algorithms are proposed to realize All-Reduce pattern and are implemented in communication frameworks such as Intel oneCCL [22] or NVidia NCCL [29]. Fig. 3.b shows an example of the ringbased All-Reduce algorithm running on four NPUs. Assume the initial data residing on each NPU is N and there are P NPUs participating in the communication. In general, in a ring All-Reduce each NPU sends out $\frac{2N}{P}$ communication data to the network: $\frac{N}{P}$ during the Reduce-Scatter phase during P-1 steps, and another $\frac{N}{P}$ during the All-Gather during another P-1 steps. Fig. 3.b shows the special case when P=4. Moreover, the optimal algorithm is usually dependent on the physical topology and also the communication size [37].

For example, a physical ring topology connecting NPUs is a natural fit for ring-based algorithms. Communication size also plays a role in determining the best algorithm to be employed as previous methods showed [37]. Hence, communication libraries dynamically decide which algorithms to use based on the underlying physical topologies and communication sizes. Such basic collective algorithms provide a basis to design more complex and tuned algorithms that are optimized for multi-dimensional network topologies, as we describe next.

C. Multi-Rail Hierarchical Collective Comm. Algorithms

As stated in Sec. II-B, the optimal collective algorithm depends on the physical topology. Hence, the basic algorithms are not a good fit when having multi-dimensional physical networks

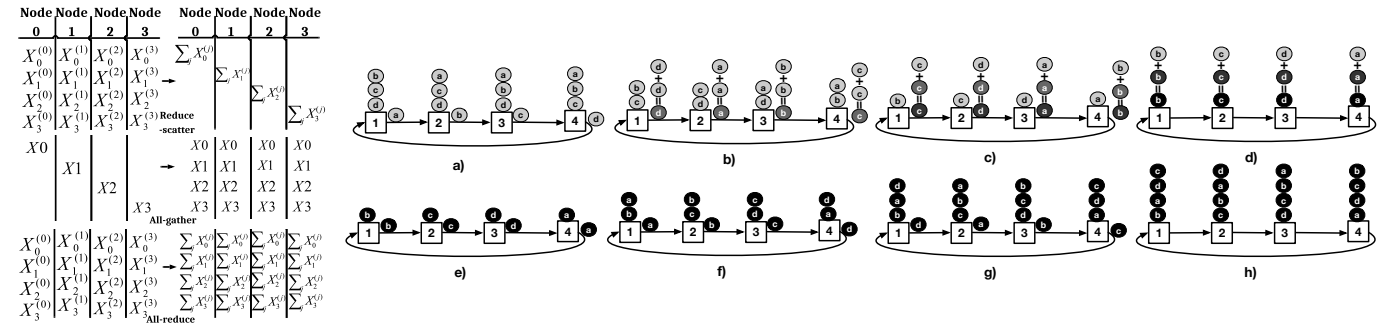
with variable BW and latencies in each dimension. This is because the collective algorithms are inherently synchronous and in this case, the links with the least BW will become the bottleneck, making other high-BW links underutilized. To cope with this problem, recent methods proposed multi-rail hierarchical algorithms to exploit the different dimension BW and latency of multi-dimensional networks [17]. Suppose the physical topology has *D* dimensions as shown in Fig. 1.a, the All-Reduce algorithm breaks into the following pipeline stages:

- A sequence of Reduce-Scatter stages starting from dim1 and ending at dimD (D stages in total). After these stages, data is globally Reduce-Scattered across all NPUs.
- Next, a sequence of All-Gather stages are performed in the reverse order (*D* stages in total); starting from dim*D* and ending at dim1.

The Reduce-Scatter/All-Gather algorithm for each stage is a basic collective algorithm described in Sec. II-B and is independently selected by the collective scheduler [29], [22] to best suit each physical dimension. For e.g., a topology with rings in the first dimension and switches in the second dimension may run ring-based and halving-doubling algorithms, respectively.

Fig. 1.b and Fig. 1.c show two examples of how this All-Reduce algorithm is applied on a 2-dimensional network. In both examples, the first dimension comprises the NPUs with the same color, meaning that the peer NPUs for the communication is the NPUs with the same color. The second dimension is shown based on the NPUs with the same number. Throughout this paper, we use the notation $P_1 \times P_2 \times \times P_D$ to refer to the size of a multi-dimensional network where P_i is a number referring to the size of peer NPUs participating in the communication in the i'th dimension. For example, the size of both Fig. 1.b and Fig. 1.c is 4×4 .

Chunks. Communication data is usually broken into multiple chunks [29] and then these chunks are fed into this 2D-stage pipeline to keep all dimensions busy. A chunk is a portion of data to be participated in the collective, and collective algorithm can work on each chunk independently. For e.g., a 256MB All-Reduce, can be broken into four chunks of 64MB All-



(b) Example of All-Reduce Collective Communication Algorithm

Fig. 3: (a) The Mathematical Implications of the Reduce-Scatter, All-Gather, and All-Reduce patterns executing on four NPUs. The left part shows the initial data on each communicating NPU before the collective operation. The right part shows data residing on each NPU after the completion of the collective operation. (b) An example of the ring All-Reduce algorithm to perform the All-Reduce pattern. Steps adperform Reduce-Scatter pattern and steps e-g perform All-Gather pattern. Step h shows the final result.

Reduces. In this paper, we assume the size of each chunk in each stage to be the size of the corresponding chunk data residing on each NPU **before** the stage begins. Similar to the explanation of Sec. II-A, each chunk size changes after each stage of Reduce-Scatter/All-Gather.

(a) Collective Communication Patterns

III. MOTIVATION - NETWORK BW UNDER-UTILIZATION

As discussed in Sec. II-C, hierarchical collectives are the state-of-the-art method for the multi-dimensional networks with variable BW. However, as we identify in this work, reaching the maximum possible network utilization is quite challenging. This fact is quantitatively reflected in Fig. 2 where we observe that the baseline can only utilize 55.6% of network BW, on average. To obtain linear (perfect) speedup as we scale the number of NPUs for training, the communication overhead should remain 0% (the Inf BW case in Fig. 2). However, this is not feasible due to finite network BW resources (technology constrained in each dimension). Hence, for a given topology, the maximum achievable speedup is when BW utilization is 100% ("Ideal" in Fig. 2), and any network under-utilization diminishes the benefits of scaling.

The fundamental reason why utilizing the full BW is challenging is because *both* the chunk size and network BW change as each chunk goes to the different stages of the pipeline, making it challenging to keep the pipeline stage latencies equal. Unequal pipeline stage latencies indicate some stages do not have any chunk to process at some periods, making their corresponding network dimension underutilized.

To illustrate the problem, Fig. 4.a shows how a 256MB baseline hierarchical All-Reduce is performed on a 2-dimensional network with the second dimension having half BW of the first dimension. The collective is broken into 4×64MB chunks. There are 4 pipeline stages for performing hierarchical All-Reduce on this network: ① Reduce-Scatter on Dim 1, ② Reduce-Scatter on Dim 2, ③ All-Gather on Dim 2, ④ All-Gather on Dim 1.

A 64MB chunk size will be shrunk by $4\times$ when entering stage 2, meaning that Reduce-Scatter on the stage injects $\frac{1}{4}\times$ data to the dim2 compared to the stage 1 injecting to dim1.

However, dim2 has $\frac{1}{2} \times$ BW compared to the dim1. If we assume the 64MB Reduce-Scatter (or 16MB All-Gather) takes 1 unit of time when running on dim1, then the latency of that chunk for the stage 2 is: $\frac{0.25Data}{0.5BW} = 0.5$. Therefore, stage 2 is performing $2 \times$ faster than stage 1. Stage 3 injects the same amount of data as stage 2 and operates on the same dimension, hence its latency is similar to stage 2. Using the same argument, stage4 has the same latency as stage 1.

The faster processing of stage 2 and stage 3 means they are underutilized many times. This indicates that their corresponding network dimension (i.e. dim2) is underutilized as shown in Fig. 4.a.

We noted that the only place where the baseline algorithm can reach near 100% utilization is when the BW reduction ratio in the next dimension is proportional to the size of the current dimension. Again, consider the 4×4 system size. For the baseline system to be efficient, the BW(dim1)=4BW(dim2) because dim1 shrinks the chunk size by $4\times$. It is only in this case that stage latencies will be equal using the baseline algorithm. Any excess BW of dim2 beyond this point will be wasted, as when we showed in Fig. 4.a where BW(dim1)=2BW(dim2).

In general, this concept can be generalized to any D-dimensional network of size $P_1 \times P_2 \times \times P_D$. For the baseline to be efficient, we must have:

$$BW(\dim 1) = P_1 \times BW(\dim 2) = P_1 \times P_2 \times BW(\dim 3) = \dots = P_1 \times P_2 \times \dots \times P_{D-1} \times BW(\dim D).$$

However, this creates an unpleasant requirement to the network as a result of poor scheduling of the baseline algorithm. The underlying network dimensions can have more BW available (and in practice they have) and the algorithm must be able to utilize excess BW provided by the network dimensions.

Note that in the above example, our analysis was based on the assumption that the network BW is the primary factor that determines communication latency (which is true for large collectives). However, the concept of unbalanced stage latencies remains true even if we take into account other factors (e.g. link latency) as we show in Sec. V and Sec. VI.

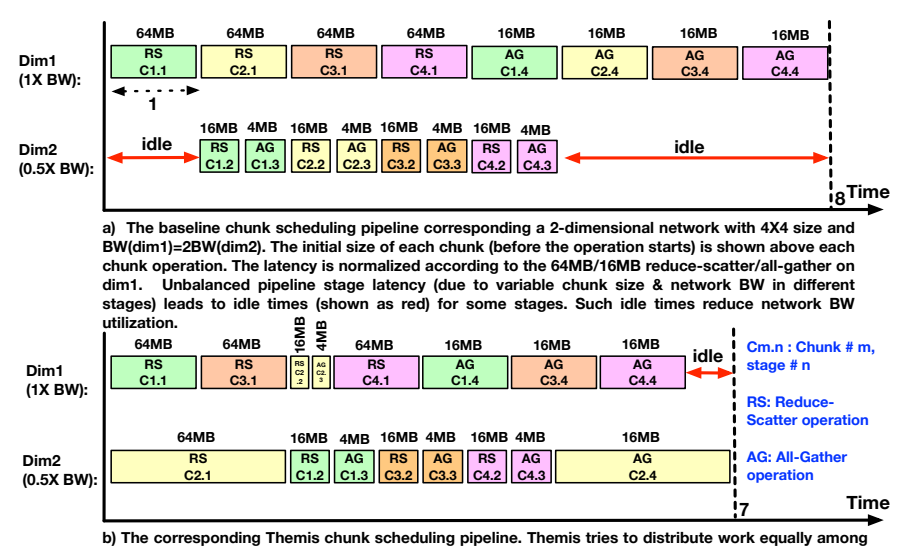


Fig. 4: The execution of a 256MB All-Reduce running on a 4×4 2-dimensional network where BW(dim1)=2BW(dim2). The All-Reduce is broken into the 4×64 MB chunks.

reduce-scatter/all-gather takes 2X more time on dim2 since dim2 has 0.5X network BW.

all dimensions, resulting in more network utilization and reduced overall latency. Note that 64MB/16MB

Themis Architecture Splitter Splitter Dim load Tracker Judate the loads Scheduler Scheduler

Fig. 5: An overview of Themis components. 1) A collective operation is requested from the upper layer training workload. 2) The collective is split into multiple equal size chunks. Steps 3-6 are performed on an individual chunk basis. 3) the current load of network dimensions (in terms of total communication latency) is retrieved from the Dim Load Tracker. 4) Scheduler sorts the dimension loads in ascending orders and the sorted list order is the schedule for the current chunk through the Latency Model. 5) Based on the schedule generated, Scheduler finds out the latency of the new schedule for each dimension. 6) Scheduler updates the total loads of each dimension to take into account the load of the new chunk.

IV. THEMIS

A. Overview

In this section, we present our method, called Themis, that leverages dynamic and distinct scheduling for each chunk to balance the loads across different network dimensions. Themis is specifically designed to maximize the multi-dimensional network BW for All-Reduce, Reduce-Scatter, and All-Gather patterns, the most observed communication patterns in distributed training. Themis has roots in two main observations:

Observation 1. From the algorithm and correctness point of view, there is no restriction in how each chunk should traverse the Reduce-Scatter (RS)/All-Gather (AG) stages. For example, in the case of All-Reduce on a 2-dimensional network explained in Sec. III, RS stage on the second dimension can precede the RS on the first stage. Similar ordering independence is true for AG stages. Furthermore, the ordering of RS stages can be different than AG stages. The only synchronization point is that RS stages should be finished before starting the AG stages. Thus, the following 4 different schedules are all possible for the All-Reduce collective on a 2-dimensional topology:

- 1) (i) RS on dim1, (ii) RS on dim2, (iii) AG on dim2, (iv) AG on dim1 (this is the baseline scheduling).
- (i) RS on dim2, (ii) RS on dim1, (iii) AG on dim2, (iv) AG on dim1.
- 3) (i) RS on dim1, (ii) RS on dim2, (iii) AG on dim1, (iv) AG on dim2.
- 4) (i) RS on dim2, (ii) RS on dim1, (iii) AG on dim1, (iv) AG on dim2.

In general, for any N-dimensional network, there are $N! \times N!$ valid ways to schedule an All-Reduce data chunk (N! for Reduce-Scatter/All-Gather only chunk).

Observation 2. Different chunks can have different schedules. Hence, if we divide a collective to C chunks, the space of all possible schedules for all chunks on an N-dimensional network is $(N! \times N!)^C$ for All-Reduce $(N!^C)$ for Reduce-Scatter/All-Gather), indicating the exponential growth as the network dimensions and the number of chunks increase.

Themis, like the baseline hierarchical algorithm, assumes that Reduce-Scatter/All-Gather per each dimension can be any basic collective algorithm that suits that particular dimension. Fig. 5 shows the general overview of Themis. Splitter component simply divides the collective into multiple equallysized chunks. Dim Load Tracker maintains the load of each network dimension in terms of total communication time of the chunks when executing on that dimension. Latency Model predicts the Reduce-Scatter/All-Gather communication time for a given chunk size running on any network dimension. Latency *Model* can be based on the analytical model or real system measurement data provided to the Themis (More details in Sec. IV-B). Finally, Scheduler generates a dynamic schedule for each chunk based on the information provided by Dim Load Tracker and Latency Model. Fig. 5 also shows the series of steps when a new collective communication is issued from the training workload layer. We describe its workflow next.

B. Themis Algorithm

In Sec. IV-A we showed how the space of available schedules grows exponentially. Therefore, it is not practical to search all possible schedules, even for modest network and chunks granularity². Instead, Themis is a type of greedy algorithm that tries to schedule new chunks in a way that puts more load (in terms of communication time) on the dimension with a lower load.

²For example, when N=3, and C=8, all the space of all All-Reduce schedules is $(3!*3!)^8 = 2821109907456$.

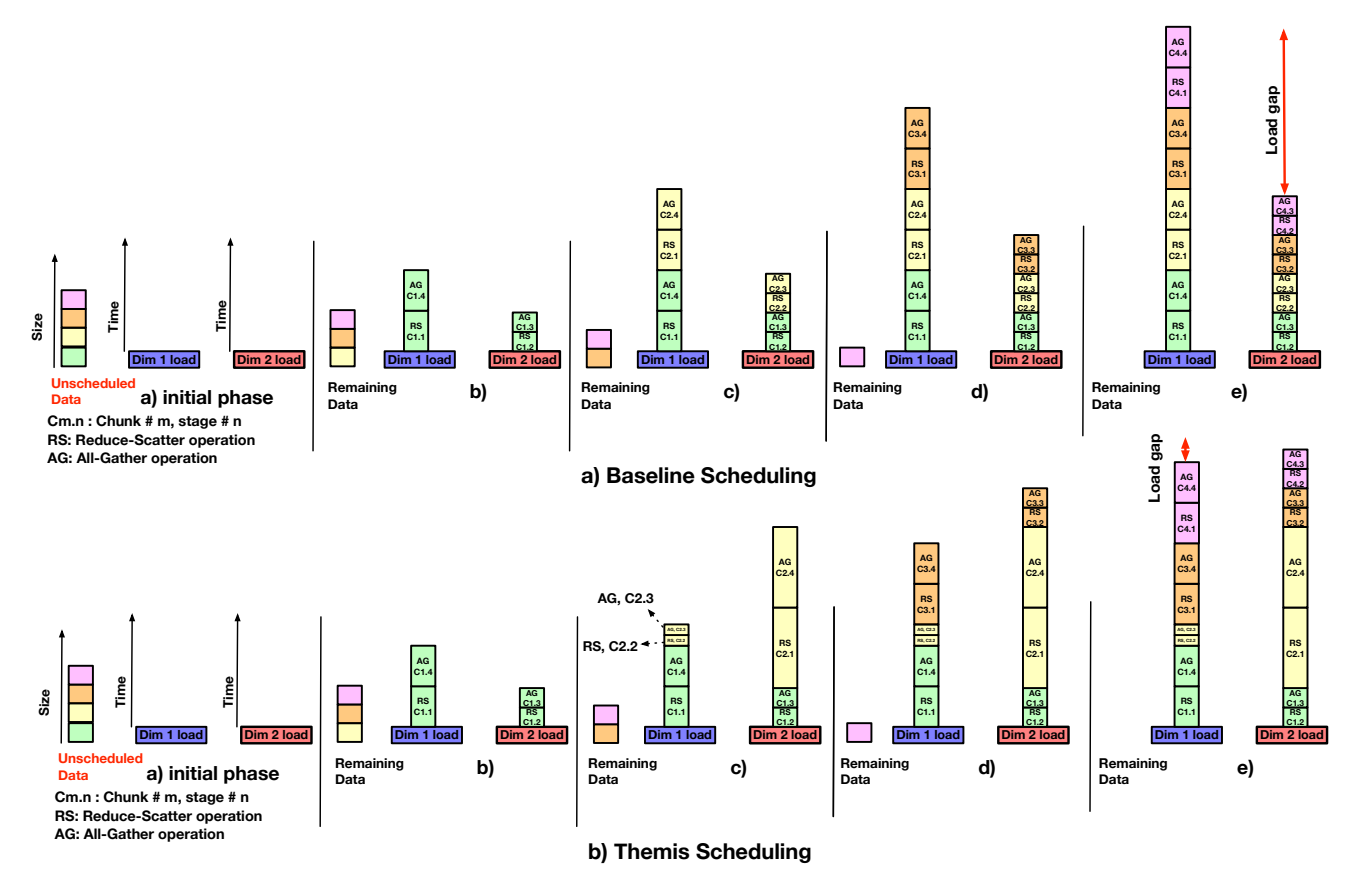


Fig. 6: An example of Baseline Scheduling vs. Themis Scheduling corresponding to the chunk scheduling problem of Fig. 4. Each of the steps b-d shows scheduling for one chunk. Dim load shows the total communication time of each dimension. As shown in the figure, baseline scheduling always uses a constant schedule for all chunks, resulting in the underutilization of abundant BW provided by dim2. However, Themis uses a greedy scheme to schedule new chunks in a way that puts more load on the dimensions with lower loads. In Themis: step b) all dim loads are zero, thus, the first chunk schedule is similar to the baseline. In step c) dim2 has a lower load, hence the chunk scheduling starts from dim2 to fill the gap with dim1. In step d) and step e) Chunk schedule starts from dim1 to fill the gap with the overloaded dim2.

Themis leverages the two observations explained in Sec. IV-A for a more flexible scheduling. Algorithm 1 shows the pseudocode for Themis. The SCHEDULE COLLECTIVE procedure (line1) is called whenever a new collective is requested by the training workload. Lines 2-4 are for initialization. The for loop in line 5 is for chunking the data while the lines 6-14 are executed to call the scheduler to determine the schedule of each chunk through SCHEDULER.SCHEDULE procedure. Note that Themis assumes the All-Gather schedule is the reverse order of obtained Reduce-Scatter schedule (line 9), similar to the baseline scheduling. The scheduler first retrieves the current loads of all network dimensions via the Dim Load Tracker component (line 19). Dim Load Tracker is simply a list that contains total load (chunk runtimes predicted by the latency model) that is placed on each dimension by the current schedules of the chunks. Then, Themis gets the index of dimensions sorted from least (most) load to most (least) load if the collective type is Reduce-Scatter (All-Gather) (lines 20-28). This sorted list is the schedule for the new chunk, since such schedule increments new load on the lower-load dimensions first, leading to filling the gap between the high-load and lowload dimensions. Next, the latency model predicts the load of

the newly scheduled chunk (lines 29-30), and then Dim Load Tracker is updated (increased) accordingly (line 31). Latency model is a function that inputs chunk size, network dimension, and chunk operation (Reduce-Scatter/All-Gather), and returns the predicted runtime for that chunk operation running on the specific dimension. Then, the scheduling process for the next chunk begins.

To design a distributed chunk scheduling algorithm, it is important to maintain scheduling consistency across all NPUs, since inconsistent (different) scheduling between NPUs results in deadlock. To guarantee consistency, we make two considerations. First, latency model is obtained offline by profiling (in our case simulating) the network performance on different dimensions and for different operations. After obtaining the latency model for a given platform, the model is replicated to all NPUs and it remains constant during the training. Second, Dim Load Tracker maintains the loads reported by the latency model and does not perform online tracking of the dimension loads. These two design choices guarantee that all NPUs have the same view of the chunk load overheads and hence, produce the same schedules. We note that it is possible to implement a more accurate model by

Algorithm 1 Themis Algorithm

Inputs: CollectiveType (CT), CollectiveSize (CS), ChunksPer-Collective (CPC), TotalNPUs (P)

Output: A 2D list *Schedule*[i][] where *Schedule*[i][] gives the order of dimensions the i'th chunk should traverse for the collective.

```
1: procedure SCHEDULE COLLECTIVE(CT, CS, CPC)
2:
       DimLoadTracker.initializeToZero()
 3:
       ChunkSize=CS/CPC
4:
       i=0
       for i++<CPC do
 5:
          if CT == All - Reduce then
 6:
              RS Sch=SCHEDULER.SCHEDULE(
 7:
8:
                                          RS, ChunkSize)
 9.
              AG Sch=reverseOrder(RS Sch)
              Schedule[i][] = concatenate(RS\_Sch,AG\_Sch)
10:
11:
              Schedule[i][]=SCHEDULER.SCHEDULE(
12:
                                         CT, ChunkSize)
13:
          end if
14:
15:
       end for
       return Schedule
16:
17: end procedure
18: procedure SCHEDULER.SCHEDULE(CT, ChunkSize)
   Schedules a chunk
19:
       loads=DimLoadTracker.getLoads()
20:
       if CT == Reduce - Scatter then
          schedule=getIndexOfSortedList(
21:
                               loads, ascending)
22:
23:
       else
          if CT == All - Gather then
24:
              schedule=getIndexOfSortedList(
25:
                                   loads, descending)
26:
          end if
27:
       end if
28:
29:
       newLoad=LatencyModel.calcLoads(
30:
                                chunkSize, schedule, CT)
31:
       DimLoadTracker.update(newLoad)
       return schedule
32:
33: end procedure
```

online tracking of the latencies and loads at the expenses of introducing synchronization mechanism between NPUs. However, similar to other studies that rely on offline analysis for designing new collectives [40], [25], we found an offline model to be sufficient to achieve good performance (Sec. VI)³.

Fig. 6 shows how baseline vs. Themis scheduling works (i.e. assigns schedules) for the example of Fig. 4. As Fig. 6 shows, the baseline scheduling scheme always assigns a constant schedule for all chunks, hence, the gap between dim1 and dim2 preserves as new chunks are scheduled. However, Themis schedules the chunks differently to balance the dimension loads. In this example, Themis schedules the second chunk to start

from dim2 to fill the gap between dim1 and dim2 (step c). After that, the last two chunks start from dim1 to fill the gap of dim1 with now overloaded dim2 (steps d&e).

Fig. 4.b shows the Themis time diagram that is based on the schedule generated in Fig. 6.b. As Fig. 4.b shows, such dimension load balancing results in better network utilization and reduced total communication time. We used a 2-dimensional example for simplicity. However, in general, the lack of ability to utilize the network BW in the baseline scheduling is more pronounced as the number of network dimensions and available extra BW of dimensions increase. its als

C. Intra-Dimension Chunk Scheduling

So far, we have discussed how Themis schedules chunks across different dimensions to balance the loads (inter-dimension scheduling). The other important question to answer is how different chunks within a dimension are ordered for processing because at any given point there might be multiple chunks available for each dimension. Adverse intra-dimension scheduling can lead to starvation of some dimensions since their, yet to come, chunks are stuck within the queues of other dimensions.

We found out that in the baseline scheduling scheme, intradimension scheduling has minimal effects on the performance due to the identical schedule of all chunks. In other words, no matter how each dimension selects chunks to process, the average BW utilization remains fixed. The only difference is in the periods of times where the dimensions are utilized. Moreover, a monotonic schedule means each network dimension always receives the same chunk sizes. Hence, we assume the baseline scheme uses a simple FIFO-based intra-dimension chunk execution.

But for Themis, chunk intra-scheduling is important due to the different schedules of chunks, that result to variable chunk size per dimension. We empirically found the best policy to be Smallest-Chunk-First (SCF). The underlying intuition is that processing smaller chunks takes a shorter time and allows the chunk to be fed to other dimensions faster. Also note that if the chunk is small, processing one chunk per dimension underutilizes the network BW since small messages cannot saturate the given BW (e.g. due to the link latency). Hence, in this case, multiple chunks per dimension (if available) should be run in parallel to fully saturate a dimension's available BW.

V. METHODOLOGY

In this section, we provide our methodology and the target systems and workloads to evaluate Themis and baseline.

A. Training Platforms and Workloads

Simulation Infrastructure. We use Facebook and Intel-supported ASTRA-SIM simulator [1], [34] to implement our scheme and compare it with the baseline system. ASTRA-SIM provides the flexibility to define various large-scale hierarchical training platforms, enabling us to demonstrate the efficiency of Themis on both current and future platforms.

³Due to the inherent synchronization of the collective operations, there is a very little variation across NPUs on the actual loads sensed by each collective. Hence, an offline model can predict the loads very accurately.

TABLE I: List of target topologies and their BW/latency configurations per each dimension. Naming convention starts with number of dimensions followed by dimension topology time in increasing order. For example, 3D-FC_Ring_Switch means a 3-dim topology where dim1 is Fully connected, dim2 is ring, and dim3 is switch. For all same type dims, then the dim type is mentioned once (e.g., 3D-Switch_homo).

Name	NPUs	Size	BW/Link (Gb/s)	#Links/NPU	Aggr BW/NPU (Gb/s)	Link Latency (ns)
2D-Switch	1024	16×64	(200, 400)	(4, 1)	(800, 400)	500
3D-Switch_homo	1024	16×8×8	(200, 200, 400)	(4, 4, 2)	(800, 800, 800)	500
3D-Switch_hetero	1024	16×8×8	(200, 200, 400)	(8, 4, 1)	(1600, 800, 400)	500
3D-FC_Ring_Switch	1024	8×16×8	(200, 200, 400)	(7, 4, 1)	(1400, 800, 400)	500
4D-FC_Ring_Ring_Switch	1024	$8 \times 4 \times 4 \times 8$	(200, 200, 200, 400)	(7, 4, 2, 1)	(1400, 800, 400, 400)	500
4D-Switch_Ring_Ring_Switch	1024	$8 \times 4 \times 4 \times 8$	(200, 200, 200, 400)	(4, 4, 4, 1)	(800, 800, 800, 400)	500

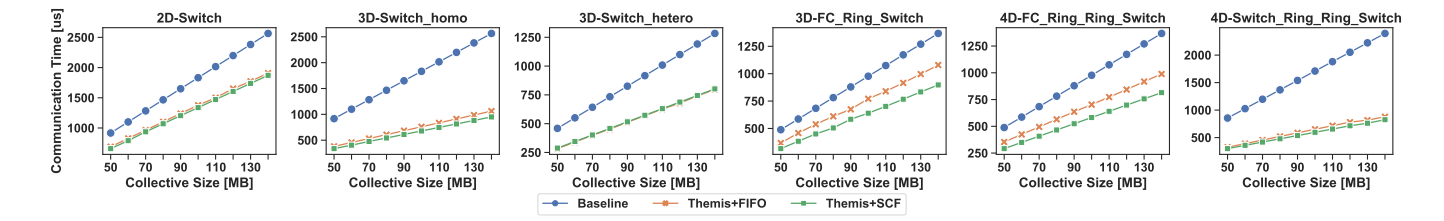
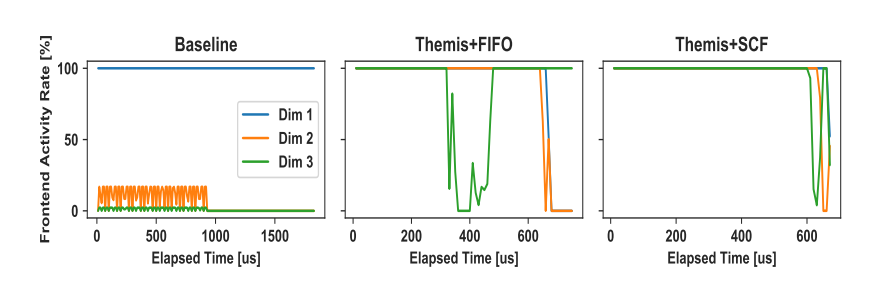


Fig. 7: Total communication time of baseline, Themis+FIFO, and Themis+SCF for different size All-Reduces. Note that Themis+FIFO uses FIFO intra-dimension chunk scheduling, while Themis+SCF uses the smallest available chunks for intra-dimension chunk execution.



Number of Chunks per Collective

Fig. 8: The average per-dimension activity rate for, Themis+FIFO, and Themis+Smallest-Chunk-First (SCF) for a 100MB All-Reduce size when running on 3D-Switch_homo topology. A dimension is called to be activated if there is at least one chunk in that dimension for processing at any given point in time. Each point in the graph shows the percentage of the times a given dimension was activated during the $10\mu s$ period.

Fig. 9: Sensitivity analysis that shows Total BW utilization for a single 100MB All-Reduce when the number of chunks per collective varies from 4 to 512. The target topologies are 3D-Switch_hetero and 4D-FC_Ring_Ring_Switch.

TABLE II: Target implemented configurations

Method	Comment			
Baseline	Baseline scheduling as explained in Sec. II-C			
Daseille	it uses FIFO intra dimension scheduling.			
Themis+FIFO	Uses FIFO intra-dimension scheduling.			
Themis+SCF	Uses SCF intra-dimension scheduling.			
Ideal	Assumes 100% BW is utilized.			
	Communication latency is simply			
	calculated by (collective size/ total BW).			

ASTRA-SIM simulates the communication performance of the distributed training workloads in detail and uses a modified version of gem5-garnet [15], [12] as its network simulator to model heterogeneous bandwidth topologies. It also supports different collective communication algorithms and different parallelization strategies. For compute times (in the case of real workloads), we use A100 [8] profiling.

Target Training Platforms & Topologies. Table I shows our target topologies, all consisting of 1024 NPUs to resemble large-scale systems. The BW and latency in each dimension

are selected according to the predicted range in the future systems [42], [4]. For the training platforms, we mostly used the flavors of the hierarchical switch-based topologies since they are the most common topologies for large-scale training [42], [30].

Today's high-performance training platforms typically used two-dimensional topologies – one to connect several NPUs within the same server node together, followed by node-to-node communication via Network Interface Cards (NICs). We model this platform through 2D-Switch configuration described in Table I. However, as workload model sizes increase [39], the need for more NPUs and higher communication bandwidth increases. There is thus a growing industry trend [42], [4], [9], [6] to increase the number of dimensions before getting to the NIC. We model three such futuristic 3-dimensional training platforms in this work as described in Table I. The first dimension (dim1) represents the intra-node dimension where NPUs on the same server are connected through a high-BW fabric. These nodes are then connected (using dedicated

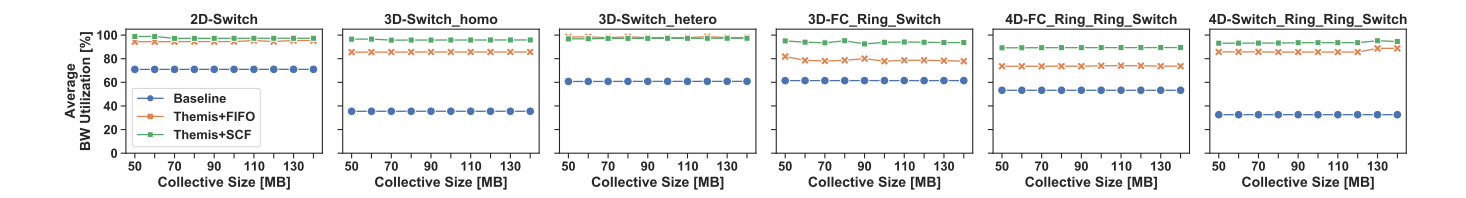


Fig. 10: Average BW utilization of baseline, Themis+FIFO, and Themis+Smallest-Chunk-First (SCF) for different size All-Reduces.

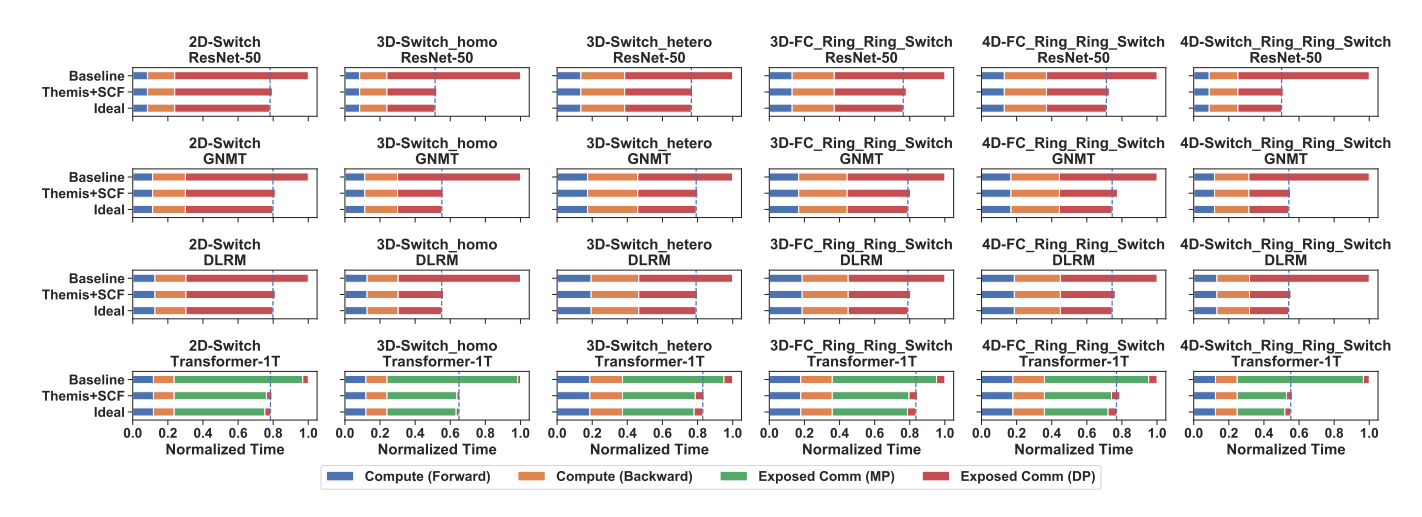


Fig. 11: Training times for 3 iterations for ResNet-50, GNMT, DLRM, and Transformer-1T running on different topologies. Training iteration consists of a forward-pass followed by a back-propagation step. The total latency is decomposed to the compute times (across all layers), plus the total exposed communication latency. Compute times stem from computation during the forward pass (blue bar) or during the backpropagation (orange bar). Exposed communication may be due to the waiting for the data-parallel communications (red bar), or model-parallel communication (green bar), as explained in Sec. V-A. For each workload, the latency of the baseline is normalized to 1.

links) through another fabric to create dim2 [42], [4], [9], [6], again, using high-BW links. In the third dimension, NPUs within dim2 are connected to the dim3 switches through (one or two) Network Interface Cards (NICs). We further expanded 3-dimensional networks by breaking the dim2 into a 2D torus topology (i.e. two consecutive ring dimensions) to create 4-dimensional networks, as shown in Table I. Hence, we create a diverse set of topologies with a different BW ratio to demonstrate the applicability of Themis on various platforms.

All-reduce Algorithm. For switch, ring, and fully-connected dimensions, We used halving-doubling [18], ring-based [16], and direct all-reduce [33] algorithms, respectively. Such algorithms are shown to be efficient and contention-free algorithms on their respective dimension type.

Target Workloads and Parallelization. Themis is a solution to maximize the BW utilization of pervasive collective communications on multi-dimensional networks. Collective communication is an integral part of any synchronous training job with an NPU-to-NPU communication mechanism. Moreover, collective usage is not limited to Training only, and has been widely used in other domains (e.g., in HPC applications and distributed inference). However, we limit the scope of our evaluations in this work to DL training given its importance.

For real workload training, we selected four DNNs from

different domains of deep learning applications: ResNet-50 [20] (from computer vision), DLRM [28] (from recommendation models), GNMT [41], and Transformer-1T (one trillion parameter) [5] (both from NLP domain). Such workloads have high ratio of communication-to-computation and hence, benefit most from applying Themis.

In terms of parallelization strategy, ResNet-50 and GNMT use the complete data-parallel partitioning since they can fit within single NPU's memory. DLRM uses data-parallel partitioning for its MLP layers, while its sparse-features (embedding tables) are partitioned in model-parallel. The model size of DLRM is chosen based on [33]. To reduce the memory requirements for DNN training, Transformer-1T uses Microsoft Zero optimizer stage 2 [32]. Transformer-1T is partitioned in a model-parallel manner across the first dimensions up to 128 NPUs, and data-parallel across the remaining dimensions. The reason is that a single NPU memory is usually within the range of 48-64GB [4], [42]. Thereby, the entire parameters of Transformer-1T (even after applying Zero optimizer) can not fit within a single NPU, requiring model-parallel to split the model.

B. Target Configurations

Target Scheduling Configurations.. Table II shows the methods we implement. The baseline uses FIFO intradimension policy as different intra-dimension policies have no effects on its performance (discussed in Sec. IV-C). To decompose the effect of inter-dimension and intra-dimension scheduling, we presented two flavors of Themis: i) Themis+FIFO that uses the default FIFO intra-dimension scheduling policy, and ii) Themis+Smallest-Chunk-First (SCF) with optimized SCF intra-dimension policy. Moreover, for the real workloads, we implement an Ideal method that assumes 100% network BW utilization. Ideal method determines the upper bound for maximum achievable speed-up and guarantees that no chunk scheduling scheme can exceed its performance.

Themis Parameter Values. According to the Fig. 5 and Algorithm 1, Themis has two important parameters to be set: i) latency model component and ii) the number of chunks per each collective. To configure the latency model and for better accuracy, we first simulated various sized Reduce-Scatter/All-Gather collectives to determine the communication time (i.e. load) for different size collectives on each dimension. The latency model uses this data to interpolate other communication times if requested by the algorithm. Unless mentioned otherwise, we set the number of chunks per collective to be 64 in all our experiments for both the baseline vs. Themis.

C. Metric of Evaluation

We use different metrics to evaluate our scheme in Sec. IV. For the first part of the Sec. IV that is about single collective performance (with no workload computation), we mainly focus on the total communication runtime, average network BW utilization, and dimension activity. Dimension activity refers to the percentage of the times where each dimension at least has one chunk to process.

For real workloads our main metric is *total computation* + *exposed communication*. Exposed communication refers to the communication overhead of the training time where the training workload is waiting for the communication to be finished.

According to the default implementation on training frameworks (e.g., PyTorch [10], TensorFlow [11]), this case for data-parallel partitioning is at the end of back-propagation, where NPUs communicate their locally computed weight gradients through All-Reduce, updating their model parameters before next iteration starts.

Handling the model-parallel communication case is different in DLRM vs. Transformer-1T. For DLRM, its sparse features form a concurrent path with bottom-MLP layers and hence, its model-parallel communication (in terms of All-to-All collective operation) is performed in parallel with forward-pass, and back-propagation of bottom-MLPs. We only wait for the embedding communication operation (i.e. all-to-all) before entering the top-MLP layers in forward-pass, and after finishing the back-propagation to update the embedding. In the case of Transformer-1T, the output-activations/input-gradients of a (model-parallel) layer must be communicated (through All-Reduce or All-Gather, depending on the layer type

in Transformer) during forward-pass/back-propagation before processing the next layer. In all cases, the summation of the (total computation + exposed communication) then determines the training iteration time.

VI. RESULTS

In Sec. VI-A, we first present the single collective microbenchmark results and dive deep into the reasons for Themis showing benefits over baseline scheduling scheme. Next, in Sec. VI-B we present the end-to-end training iteration results for real workloads such as ResNet-50, GNMT, DLRM, and Transformer-1T. Finally, in Sec. VI-C, we give insights on how next generation networks should be designed in terms of BW distribution for distributed training.

A. Microbenchmark Results

Fig. 7 shows the All-Reduce communication results of baseline and Themis. As Fig. 7 shows, applying Themis significantly reduces the communication time. When averaging across all topologies and comm sizes, Themis+FIFO and Themis+SCF reduces the communication time by $1.70\times$ and $1.88\times$ over the baseline, respectively.

To shed light on the reason behind Themis benefits, Fig. 8 shows the the per-dimension activity rates for a 100MB All-Reduce on 3D-Switch homo. A network dimension is called to have activity if there is at least one chunk in that dimension for processing at any given point of time. As can be seen, in the baseline system dim2 and dim3 show significant underutilization. The reason is dim1 is the bottleneck stage in the baseline pipeline scheduling and the unbalanced stage latencies result in underutilization. Both Themis+FIFO and Themis+SCF significantly balance the loads and improve the utilization of dim2 and dim3. An interesting point about Themis+FIFO is the occasional underutilization of different dimensions. This is due to the inefficient FIFO intra-dimension chunk processing that leads to the starvation of some chunks as discussed in Sec. IV-C. Themis+SCF further reduces the starvation problem as can be seen in Fig. 8.

As Fig. 7 suggests, the amount of speed-up obtained by Themis varies by the topology. The speed-up depends on the amount of underutilization in the baseline scheduling. For example, in the case of 3D-Switch_homo, and according to the discussion in Sec. III, the baseline was able to achieve near optimal performance if:

$$BW(dim1) = 16(dim2) = 128BW(dim3)$$

According to the Fig. 8, dim1 is the bottleneck. Therefore, in the case of 3D-Switch_homo, if we substitute BW(dim1) with 800Gbps, then we have:

$$800\text{Gbps}_{\text{dim}1} = 16 \times 50\text{Gbps}_{\text{dim}2} = 128 \times 6.25\text{Gbps}_{\text{dim}3}$$

Hence, 750Gbps of dim2 and 793.75Gbps of dim3 are underutilized by the baseline scheduling for 3D-Switch_homo. Fig. 10 shows the average network utilization for variable size All-Reduce sizes. On average and across all topologies, baseline, Themis+FIFO, and Themis+SCF can achieve 52.43%,

86.23%, and 94.61% of the average network BW utilization, respectively. This indicates that Themis is an efficient method that can exploit and leverage almost all underutilized opportunities which exist in the baseline, leaving less room for further optimizations.

Next, we study the effect of chunk granularity on the performance of Themis. Fig. 9 shows the BW utilization for different number chunk granularities for baseline and Themis, when running on 3D-Switch_hetero and 4D-FC_Ring_Ring_Switch topologies. Other topologies are not included due to space limitations. For the baseline, dim1 is the bottleneck (on both topologies) and the latency is mostly determined by the rate dim1 receives the chunks to process. Since in the baseline scheduling, dim1 is always the first dimension to receive the chunks, changing the chunk granularity does not significantly affect its performance. However, increasing the number of chunks (decreasing chunk size) enables Themis to better balance the loads across the dimensions. When increasing the chunks from 4 to 512, BW utilization for Themis+SCF (Themis+FIFO) increases from 58.54% (45.48%) to 97.90% (97.05%) on average across the two topologies. We picked the default number of chunks to be 64 that achieve ~95% BW utilization for the microbenchmark workload, when averaging across all of our target topologies.

As can be seen in Fig. 9, at some points, increasing chunks modestly reduces the BW utilization for Themis. This is mainly because of the starvation case discussed earlier. However, Themis+SCF shows stable behavior starting from 32 chunks on all of our tested topologies.

B. Real Workload Results

In this section, we present real workload results to find the effect of Themis on the total end-to-end training iteration times. Here, we only use Themis+SCF configuration since it was shown to be the better approach in Sec. VI-A. Fig. 11 shows the training iteration times that are decomposed into total compute time and total exposed communication time.

For training, back-propagation computation usually takes longer since it needs to compute for both weight gradients and input gradients, compared to the forward-pass that only involves forward computation. However, this is not the case for Transformer-1T since it consists of forward-in-back-propagation steps, as a result of Zero optimizer, that is counted towards forward-pass in Fig. 11.

As Fig. 11 shows, ResNet-50 and GNMT only experience data-parallel exposed communication since they are distributed in pure data-parallel. An interesting point is about DLRM where it has a hybrid (data+model parallel as explained in Sec. V-A) parallelism, but only the data-parallel communication is counted towards exposed communication. This is because model-parallel communication (All-To-All) is overlapped with the forward-pass, back-propagation operations of bottom-MLP layers. In Transformer-1T the model-parallel communication is the dominant factor. Also, note that the data-parallel communication of Transformer-1T uses only the last network dimension in all of the topologies. This indicates that there is

only one scheduling possible for data-parallel communication of Transformer-1T, meaning that baseline and Themis have the same performance for this portion of the exposed communication. When averaging across all topologies and workloads, applying Themis reduces the exposed communication time by $1.81\times$. The speedup is close to the Ideal system that reduces the exposed communication time by $1.87\times$, on average.

Such reduction in exposed communication leads to the reduction in overall training time as well. However, the overall training iteration benefit follows Amdahl's law [13] and depends on the current ratio between the exposed communication and total computation. When averaging across all topologies, Themis reduces the training iteration time by $1.49\times$, $1.41\times$, $1.42\times$, and $1.35\times$ for ResNet-50, GNMT, DLRM, and Transformer-1T, respectively. On the other hand, the Ideal system achieves training iteration speed-up of $1.51\times$, $1.44\times$, $1.44\times$, and $1.37\times$ for ResNet-50, GNMT, DLRM, and Transformer-1T, respectively. Overall, Themis is close to the ideal system, leaving little opportunity for further optimization.

C. Insights for Future System Design

Throughout this paper, we showed how Themis can drive the BW of all network dimensions. This raises the question that how architects and system engineers should distribute the network BW across different network dimensions in the first place, and whether some design points should be prohibited. Consider any two dimensions dimK and dimL of the network, where K<L and P_I to be the network size in dimI. In this section, we explain three different scenarios for BW distribution across these two network dimensions, depending on the BW provision for dimL:

Just Enough BW Scenario. Here, the baseline (and Themis) scheduling algorithm can fully utilize the network. As explained in Sec. III, the BW distribution should be:

$$BW(dimK) = P_K \times P_{K+1} \times \times P_{L-1} \times BW(dimL)$$

In this case, the chunk size ratio is proportional to the BW ratio of the two dimensions. Hence, the baseline algorithm is sufficient to utilize both dimensions.

OverProvisioned BW Scenario. Here, the baseline fails to use all available network BW, while Themis can fully utilize the network. :

$$BW(dimK) < P_K \times P_{K+1} \times \times P_{L-1} \times BW(dimL)$$

As explained in Sec. III, this is the case where the baseline can not utilize the full BW of dimL. While Themis redistributes the loads that results into full utilization of all dimensions.

UnderProvisioned BW Scenario. In this case there may be no scheduling algorithm that can fully drive both dimensions:

$$BW(dimK) > P_K \times P_{K+1} \times \times P_{L-1} \times BW(dimL)$$

In such BW distribution and with baseline scheduling, dimK is underutilized while it has $P_K \times P_{K+1} \times \times P_{L-1}$ more loads, compared to dimL (dimL has underprovisioned BW).

To fully utilize both dimensions, any redistribution of chunks should increase the load difference of dimK compared to dimL. However, this only can happen efficiently if dimK has overprovisioned BW compared to some other dimension and this might not always be the case. For example, in a simple 2-dimensional network case where K=1, L=2, and L is underprovisioned, there is no scheduling that can fully utilize both dimensions, since the baseline scheduling already puts the highest load on dimK, and any other scheduling reduces the load of dimK and increases the load of dimL. Thus, such design points should be prohibited.

VII. CONCLUSION

In this paper, We showed that hierarchical multi-stage collective algorithms fail to saturate the available network BW due to the different pipeline stage latencies induced by variable chunk sizes and network characteristics in each network dimension. We proposed Themis as a solution to improve the BW utilization by dynamically scheduling the chunks to balance the loads across different network dimensions. Themis improves the end-to-end training iteration performance of real workloads, such as ResNet-50, GNMT, DLRM, and Transformer-1T, by $1.49 \times (1.96 \times \text{max})$, $1.41 \times (1.81 \times \text{max})$, $1.42 \times (1.80 \times \text{max})$, and $1.35 \times (1.78 \times \text{max})$, respectively.

REFERENCES

- "ASTRA-SIM: Enabling SW/HW Co-Design Exploration for Distributed DL Training Platforms," https://github.com/astra-sim/astra-sim.git.
- [2] "Cloud TPU," https://cloud.google.com/tpu.
- [3] "Fully Sharded Data Parallel: faster AI training with fewer GPUs," https://engineering.fb.com/2021/07/15/open-source/fsdp.
- [4] "Gaudi Training Platfrom White Paper," https://habana.ai/wp-content/ uploads/2019/06/Habana-Gaudi-Training-Platform-whitepaper.pdf.
- [5] "Google Open-Sources Trillion-Parameter AI Language Model Switch Transformer," https://www.infoq.com/news/2021/02/google-trillion-parameter-ai/.
- [6] "Graphcore," https://www.graphcore.ai/.
- [7] "Habana," https://habana.ai.
- [8] "NVIDIA A100 TENSOR CORE GPU," https://www.nvidia.com/enus/data-center/a100/.
- [9] "NVIDIA DGX SuperPOD: Instant Infrastructure for AI Leadership," https://resources.nvidia.com/en-us-auto-datacenter/nvpod-superpod-wp-09
- [10] "PyTorch," https://pytorch.org/.
- [11] "TensorFlow," https://www.tensorflow.org/.
- [12] N. Agarwal, T. Krishna, L. Peh, and N. K. Jha, "Garnet: A detailed on-chip network model inside a full-system simulator," in 2009 IEEE International Symposium on Performance Analysis of Systems and Software, 2009, pp. 33–42.
- [13] G. M. Amdahl, "Validity of the single processor approach to achieving large scale computing capabilities," in *Proceedings of the April 18-20*, 1967, Spring Joint Computer Conference, ser. AFIPS '67 (Spring). New York, NY, USA: Association for Computing Machinery, 1967, p. 483–485. [Online]. Available: https://doi.org/10.1145/1465482.1465560
- [14] D. Amodei and D. Hernandez, "Ai and compute," 2018. [Online]. Available: https://openai.com/blog/ai-and-compute/
- [15] N. Binkert, B. Beckmann, G. Black, S. K. Reinhardt, A. Saidi, A. Basu, J. Hestness, D. R. Hower, T. Krishna, S. Sardashti, R. Sen, K. Sewell, M. Shoaib, N. Vaish, M. D. Hill, and D. A. Wood, "The gem5 simulator," SIGARCH Comput. Archit. News, vol. 39, no. 2, p. 1–7, Aug. 2011. [Online]. Available: https://doi.org/10.1145/2024716.2024718
- [16] E. Chan, R. van de Geijn, W. Gropp, and R. Thakur, "Collective communication on architectures that support simultaneous communication over multiple links," in *Proceedings of the Eleventh ACM SIGPLAN Symposium on Principles and Practice of Parallel Programming*, ser. PPoPP '06. New York, NY, USA: ACM, 2006, pp. 2–11. [Online]. Available: http://doi.acm.org/10.1145/1122971.1122975

- [17] M. Cho, U. Finkler, M. Serrano, D. Kung, and H. Hunter, "Blueconnect: Decomposing all-reduce for deep learning on heterogeneous network hierarchy," *IBM Journal of Research and Development*, vol. 63, no. 6, pp. 1:1–1:11, 2019.
- [18] J. Dong, Z. Cao, T. Zhang, J. Ye, S. Wang, F. Feng, L. Zhao, X. Liu, L. Song, L. Peng, Y. Guo, X. Jiang, L. Tang, Y. Du, Y. Zhang, P. Pan, and Y. Xie, "Eflops: Algorithm and system co-design for a high performance distributed training platform," in 2020 IEEE International Symposium on High Performance Computer Architecture (HPCA), 2020, pp. 610–622.
- [19] A. Harlap, D. Narayanan, A. Phanishayee, V. Seshadri, N. Devanur, G. Ganger, and P. Gibbons, "Pipedream: Fast and efficient pipeline parallel dnn training," 2018.
- [20] K. He, X. Zhang, S. Ren, and J. Sun, "Deep residual learning for image recognition," *CoRR*, vol. abs/1512.03385, 2015. [Online]. Available: http://arxiv.org/abs/1512.03385
- [21] Y. Huang, Y. Cheng, A. Bapna, O. Firat, M. X. Chen, D. Chen, H. Lee, J. Ngiam, Q. V. Le, Y. Wu, and Z. Chen, "Gpipe: Efficient training of giant neural networks using pipeline parallelism," 2019.
- [22] Intel, "Intel oneAPI Collective Communications Library," 2020. [Online]. Available: https://software.intel.com/content/www/us/en/develop/tools/oneapi/components/oneccl.html
- [23] X. Jia, S. Song, W. He, Y. Wang, H. Rong, F. Zhou, L. Xie, Z. Guo, Y. Yang, L. Yu, T. Chen, G. Hu, S. Shi, and X. Chu, "Highly scalable deep learning training system with mixed-precision: Training imagenet in four minutes," 2018.
- [24] B. Klenk, N. Jiang, G. Thorson, and L. Dennison, "An in-network architecture for accelerating shared-memory multiprocessor collectives," in 2020 ACM/IEEE 47th Annual International Symposium on Computer Architecture (ISCA), 2020, pp. 996–1009.
- [25] R. Kobus, D. Jünger, C. Hundt, and B. Schmidt, "Gossip: Efficient communication primitives for multi-gpu systems," in *Proceedings of* the 48th International Conference on Parallel Processing, ser. ICPP 2019. New York, NY, USA: Association for Computing Machinery, 2019. [Online]. Available: https://doi.org/10.1145/3337821.3337889
- [26] Y. Li, I.-J. Liu, Y. Yuan, D. Chen, A. Schwing, and J. Huang, "Accelerating distributed reinforcement learning with in-switch computing," in *Proceedings of the 46th International Symposium* on Computer Architecture, ser. ISCA '19. New York, NY, USA: Association for Computing Machinery, 2019, p. 279–291. [Online]. Available: https://doi.org/10.1145/3307650.3322259
- [27] H. Mikami, H. Suganuma, P. U-chupala, Y. Tanaka, and Y. Kageyama, "Imagenet/resnet-50 training in 224 seconds," 11 2018.
- [28] M. Naumov, D. Mudigere, H. M. Shi, J. Huang, N. Sundaraman, J. Park, X. Wang, U. Gupta, C. Wu, A. G. Azzolini, D. Dzhulgakov, A. Mallevich, I. Cherniavskii, Y. Lu, R. Krishnamoorthi, A. Yu, V. Kondratenko, S. Pereira, X. Chen, W. Chen, V. Rao, B. Jia, L. Xiong, and M. Smelyanskiy, "Deep learning recommendation model for personalization and recommendation systems," *CoRR*, vol. abs/1906.00091, 2019. [Online]. Available: http://arxiv.org/abs/1906.00091
- [29] NVIDIA, "NVIDIA Collective Communication Library (NCCL)," 2017. [Online]. Available: https://developer.nvidia.com/nccl
- [30] NVIDIA, "NVIDIA DGX-2," 2019. [Online]. Available: https://www.nvidia.com/en-us/data-center/dgx-2/
- [31] P. Patarasuk and X. Yuan, "Bandwidth optimal all-reduce algorithms for clusters of workstations," *J. Parallel Distrib. Comput.*, vol. 69, no. 2, pp. 117–124, Feb. 2009. [Online]. Available: http://dx.doi.org/10.1016/j.jpdc. 2008.09.002
- [32] S. Rajbhandari, J. Rasley, O. Ruwase, and Y. He, "Zero: Memory optimizations toward training trillion parameter models," 2020. [Online]. Available: https://arxiv.org/abs/1910.02054
- [33] S. Rashidi, P. Shurpali, S. Sridharan, N. Hassani, D. Mudigere, K. Nair, M. Smelyanski, and T. Krishna, "Scalable distributed training of recommendation models: An astra-sim + ns3 case-study with tcp/ip transport," in 2020 IEEE Symposium on High-Performance Interconnects (HOTI), 2020, pp. 33–42.
- [34] S. Rashidi, S. Sridharan, S. Srinivasan, and T. Krishna, "Astra-sim: Enabling sw/hw co-design exploration for distributed dl training platforms," in 2020 IEEE International Symposium on Performance Analysis of Systems and Software (ISPASS), 2020, pp. 81–92.
- [35] S. Rashidi, S. Sridharan, S. Srinivasan, M. Denton, A. Suresh, J. Nie, and T. Krishna, "Enabling compute-communication overlap in distributed training platforms," in *Proceedings of 48th International Symposium on Computer Architecture (ISCA)*, 2021.

- [36] A. Sapio, M. Canini, C. Ho, J. Nelson, P. Kalnis, C. Kim, A. Krishnamurthy, M. Moshref, D. R. K. Ports, and P. Richtárik, "Scaling distributed machine learning with in-network aggregation," *CoRR*, vol. abs/1903.06701, 2019. [Online]. Available: http://arxiv.org/abs/1903.06701
- [37] R. Thakur, R. Rabenseifner, and W. Gropp, "Optimization of collective communication operations in mpich," *Int. J. High Perform. Comput. Appl.*, vol. 19, no. 1, pp. 49–66, Feb. 2005. [Online]. Available: http://dx.doi.org/10.1177/1094342005051521
- [38] I. Thangakrishnan, D. Cavdar, C. Karakus, P. Ghai, Y. Selivonchyk, and C. Pruce, *Herring: Rethinking the Parameter Server at Scale for the Cloud.* IEEE Press, 2020.
- [39] A. Vaswani, N. Shazeer, N. Parmar, J. Uszkoreit, L. Jones, A. N. Gomez, L. Kaiser, and I. Polosukhin, "Attention is all you need," *CoRR*, vol. abs/1706.03762, 2017. [Online]. Available: http://arxiv.org/abs/1706.03762
- [40] G. Wang, S. Venkataraman, A. Phanishayee, N. Devanur, J. Thelin, and I. Stoica, "Blink: Fast and generic collectives for distributed ml," in *Proceedings of Machine Learning and Systems*, I. Dhillon, D. Papailiopoulos, and V. Sze, Eds., vol. 2, 2020, pp. 172–186. [Online]. Available: https://proceedings.mlsys.org/paper/2020/file/43ec517d68b6edd3015b3edc9a11367b-Paper.pdf
- [41] Y. Wu, M. Schuster, Z. Chen, Q. V. Le, M. Norouzi, W. Macherey, M. Krikun, Y. Cao, Q. Gao, K. Macherey, J. Klingner, A. Shah, M. Johnson, X. Liu, L. Kaiser, S. Gouws, Y. Kato, T. Kudo, H. Kazawa, K. Stevens, G. Kurian, N. Patil, W. Wang, C. Young, J. Smith, J. Riesa, A. Rudnick, O. Vinyals, G. Corrado, M. Hughes, and J. Dean, "Google's neural machine translation system: Bridging the gap between human and machine translation," CoRR, vol. abs/1609.08144, 2016. [Online]. Available: http://arxiv.org/abs/1609.08144
- [42] T. W. Yasaman Ghadar, "An overview of aurora, argonne's upcoming exascale system," 2020. [Online]. Available: https://ecpannualmeeting.com/assets/overview/sessions/Aurora-Public-FULL-talk-Feb-4-2020_for_posting_c.pdf